CONTROL OF FLEXIBLE ROBOT ARM

J.D. Lee, L. S. Haynes, Ben Li Wang, and Kwang-Horng Tsai*
Robot Systems Division
National Bureau of Standards
Gaithersburg, Maryland

ABSTRACT

This work is a computer simulation of the control of flexible robot arm. The dynamic equations for a single-link flexible robot arm have been derived rigorously. This arm has two degrees of freedom in rotation and one in translation so that the workspace is three-dimensional. The payload is simulated by attaching additional mass to the arm at a specified location. The governing equations of the plant and the measurements are nonlinear. The process of control is divided into two stages: coarse control and fine control. Based on the pole-placement method, a linear observer is constructed for fine control. The numerical results of several cases are presented here. The effects of damping and sampling rate are also discussed.

INTRODUCTION

Most of today's industrial robots can lift only about one twentieth of their own weight. Compare that to the human arm which can lift about ten times its own weight. The top slew velocity of a robot arm is typically around one meter per second while the top slew velocity that can be achieved by the human arm during a task such as throwing a baseball is around 48 meters per second. Although these comparisons may not be fair, the point stands that there is vast room for the improvements in the performance of robotic manipulators. One of the most elementary problem in robotics is that of accuracy. The repeatability of most of today's robots is on the order of 1 mm over the working space, the accuracy of absolute positioning (for the end effector to reach the commanded point) may be off as much as 1 cm. The present solution to the problem of accuracy is to make robot structures very stiff and rigid. Another problem in robotics is control. Nowadays, in order to position the end effector to the commanded location the angles that each of the robot's joint must assume are computed and then the joints are driven simultaneously to said angles. After the joint angles assume those computed values, the robot is presumed stiff enough so that the end effector will thus (by dead reckoning) be in the intended location. Therefore, not only the robots are built to be massive and unwieldy, the analysis and the controls in robotics are based on the assumption that the robot arm is just a collection of rigid bodies.

It is desirable to build a lightweight robot arm which has a long reach and the capability to carry heavy payload and to move rapidly. In order to meet these requirements, the robot arm has to be flexible. In other words, even the static deflection of the robot arm has to be taken into account for positioning accuracy; more importantly, the high moving speed of the arm implies the inertia forces acting on the arm are very large and the stability of the robot arm becomes a critical problem which requires the engineers to design a more sophisticated control system. In the area of control of flexible robot arm, Cannon and Schmitz [1] published the pioneer work in 1984 . In that work the mathematical modeling and the initial expreriments have been carried out to address the control of a flexible member (one link of a robot system) where the position of the end effector (tip) is controlled by measuring that position and using the measurement as a basis for applying control torque to the other end of the flexible member (joint). Also, it is worthwhile to mention the works of Harashima and Ueshiba [2], Wang and Vidyasagar [3, 4], Sangveraphunsiri [5], Book et al [6]. In all those abovementioned works, there are two things in common: the one-link robot arm, with its hub rotating about z-axis, sweeps the horizontal x-y plane; the flexible arm is modeled as a beam whose deflection is represented by a series in terms of eigenfunctions (normal modes).

In this work, the computer simulation of the control of a single-link flexible robot arm is presented. The hub of the arm can rotate about z-axis, specified by the joint angle $\theta(t)$, and y'-axis, specified by the joint angle $\phi(t)$. Also, the arm can slide along its own longitudinal axis. So that the working region of the

* Also, a graduate research assistant at Department of Mechanical Engineering, Robotics Laboratory, University of Maryland.

end effector is a three-dimensional space instead of a circle on the horizontal plane. The flexible arm is divided into a number of beam elements and then treated by finite element method to obtain the governing equations for the mechanical system. By doing so, it is more flexible and natural to incorporate payloads into the system. Moreover, it will be seen later that the system (plant) , including the measurement of the tip position, is non-linear and there is no attempt being made to linearize that.

PROBLEM DESCRIPTION

The single link robot arm being considered in this work is shown in Fig. 1. The arm consists of two parts: the hub, which is modeled as a rigid body, and the flexible beam, which is further divided into n beam elements. The flexible beam is in the shape of a slim hollow cylinder with length l, outer radius r_o, and inner radius r_i. A rectangular coordinate system (x, y, z), in which the z-axis is opposite to the direction of gravity, is employed in this work. The configuration, in which the axis of the hub, as well as the axis of the beam in its undeformed state is parallel to the x-axis, is named the home configuration. The differences in position between the deformed state and the undeformed state of the beam in the home configuration are the displacements (U_y , U_z) referring to the home configuration as indicated in the figure. Not only the flexible beam can deform, the hub can rotate about the z-axis and the y'-axis, which is perpendicular to the axis of the hub and the z-axis, and also slide along its own axis. The rotations of the arm about the z-axis and the y'-axis are specified by two time-dependent variables, $\theta(t)$ and $\phi(t)$, respectively. However, in this work, the sliding of the arm is specified by a constant parameter, d, which is determined by the given target position, as being discussed later. Since the flexible beam is modeled as n beam elements, it has

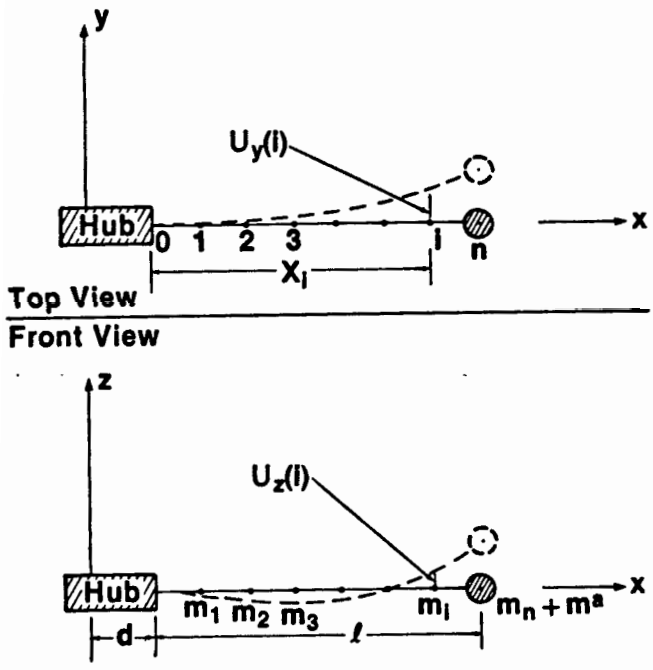

Fig. 1 Single Link Robot Arm in Its Home Configuration.

$n+1$ nodal points. The generic i-th nodal point (i = 0, 1, 2, ... , n) is associated with the lumped mass, m_i , and, referring to the home configuration, the coordinates ($X_i + d$, $U_y(i)$, $U_z(i)$). The payload is simulated by the mass attached to the end point (the n-th nodal point), m^a, as indicated in the figure. The computer software developed at NBS allows the payload to be carried at all nodal points, hence, from now on unless otherwise stated, the lumped mass, m_i , stands for the sum of the payload carried at the i-th nodal point and the mass of the beam distributed to that nodal point.

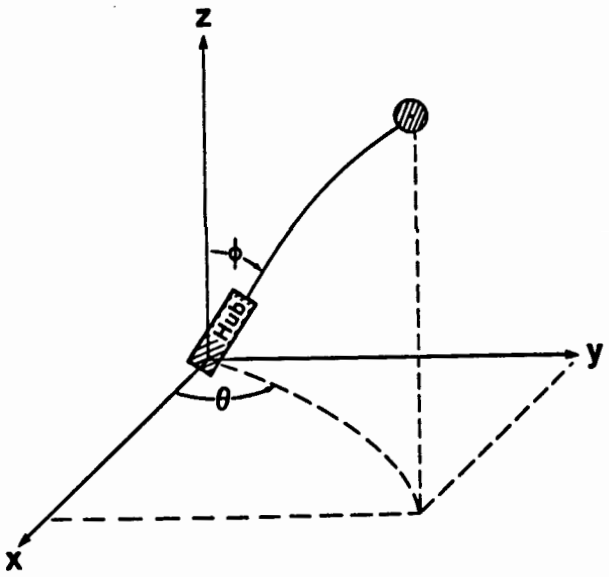

Fig. 2 Single Link Robot Arm in Its Actual Configuration

TRANSFORMATIONS

The position vector of any point on the beam, when it is in the home configuration, can be expressed as

$$\mathbf{x} \equiv \begin{bmatrix} X+d \\ U_y \\ U_z \end{bmatrix} \tag{1}$$

The rotation of the hub about the z-axis and the y'-axis transforms the arm from its home configuration to its actual configuration, as shown in Fig. 2. The transformation may be expressed by the following equation

$$\mathbf{x}^* \equiv \begin{bmatrix} x^* \\ y^* \\ z^* \end{bmatrix} = \begin{bmatrix} \sin\phi\cos\theta & -\sin\theta & -\cos\phi\cos\theta \\ \sin\phi\sin\theta & \cos\theta & -\cos\phi\sin\theta \\ \cos\phi & 0 & \sin\phi \end{bmatrix} \begin{bmatrix} X+d \\ U_y \\ U_z \end{bmatrix}$$

$$\equiv \mathbf{Q}\mathbf{x} \tag{2}$$

It is noticed that Q is an orthogonal transformation matrix which has the following properties

$$\mathbf{Q}^{-1} = \mathbf{Q}^T$$

$$\det(\mathbf{Q}) = 1 \tag{3}$$

In other words, any vector $\mathbf{V}^*$, in the actual configuration, can be transformed into $\mathbf{V}$, the corresponding vector in the home configuration, through $\mathbf{V} = \mathbf{Q}^T\mathbf{V}^*$.

Now the velocity and the acceleration, $\mathbf{v}^*$ and $\mathbf{a}^*$, can be obtained as

$$\mathbf{v}^* \equiv \frac{d\mathbf{x}^*}{dt} = \dot{\mathbf{Q}}\mathbf{x} + \mathbf{Q}\mathbf{v} \quad , \tag{4}$$

$$\mathbf{a}^* \equiv \begin{bmatrix} a_x^* \\ a_y^* \\ a_z^* \end{bmatrix} \equiv \frac{d\mathbf{v}^*}{dt}$$

$$= \ddot{\mathbf{Q}}\mathbf{x} + 2\dot{\mathbf{Q}}\mathbf{v} + \mathbf{Q}\mathbf{a} \quad , \tag{5}$$

where

$$\mathbf{v} \equiv \frac{d\mathbf{x}}{dt} = \begin{bmatrix} 0 \\ \dot{U}_y \\ \dot{U}_z \end{bmatrix} \quad , \tag{6}$$

$$\mathbf{a} \equiv \frac{d\mathbf{v}}{dt} = \begin{bmatrix} 0 \\ \ddot{U}_y \\ \ddot{U}_z \end{bmatrix} \quad . \tag{7}$$

INERTIA FORCE AND GRAVITY

The total force acting on a generic nodal point, $\mathbf{f}^*$, is equal to the sum of the inertia force and the gravitational force acting on that point, i.e. ,

$$\mathbf{f}^* = \begin{bmatrix} f_x^* \\ f_y^* \\ f_z^* \end{bmatrix} = -m \begin{bmatrix} a_x^* \\ a_y^* \\ a_z^* \end{bmatrix} + mg \begin{bmatrix} 0 \\ 0 \\ -1 \end{bmatrix} \quad , \tag{8}$$

where m is the effective mass lumped at that nodal point; and g, the constant of gravity, is equal to 9.81 m/ sec^2 . The corresponding force in the home configuration, $\mathbf{f}$, can be obtained as

$$\mathbf{f} = \begin{bmatrix} f_x \\ f_y \\ f_z \end{bmatrix} = \mathbf{Q}^T\mathbf{f}^*$$

$$= -m \left\{ \mathbf{P}\mathbf{x} + \mathbf{R}\mathbf{v} + \mathbf{a} + g \begin{bmatrix} \cos\phi \\ 0 \\ \sin\phi \end{bmatrix} \right\} \quad , \tag{9}$$

where

$$\mathbf{P} \equiv \mathbf{Q}^T\ddot{\mathbf{Q}}$$

$$= \begin{bmatrix} -\sin^2\phi\dot{\theta}^2 - \dot{\phi}^2 & -\sin\phi\ddot{\theta} & \ddot{\phi} + \sin\phi\cos\phi\dot{\theta}^2 \\ \sin\phi\ddot{\theta} + 2\cos\phi\dot{\phi}\dot{\theta} & -\dot{\theta}^2 & -\cos\phi\ddot{\theta} + 2\sin\phi\dot{\phi}\dot{\theta} \\ -\ddot{\phi} + \sin\phi\cos\phi\dot{\theta}^2 & \cos\phi\ddot{\theta} & -\cos^2\phi\dot{\theta}^2 - \dot{\phi}^2 \end{bmatrix} \quad , \tag{10}$$

$$\mathbf{R} \equiv 2\mathbf{Q}^T\dot{\mathbf{Q}}$$

$$= \begin{bmatrix} 0 & -2\sin\phi\dot{\theta} & 2\dot{\phi} \\ 2\sin\phi\dot{\theta} & 0 & -2\cos\phi\dot{\theta} \\ -2\dot{\phi} & 2\cos\phi\dot{\theta} & 0 \end{bmatrix} \quad . \tag{11}$$

For example, when $\phi = \pi/2$ and $\dot{\phi} = \ddot{\phi} = 0$, the following is obtained

$$f_y = -m \left\{ \ddot{U}_y + \ddot{\theta}(X + d) - \dot{\theta}^2 U_y \right\} \quad . \tag{12}$$

However, correspondingly, the inertia force obtained by Cannon and Schmitz [1], Harashima and Ueshiba [2], Wang and Vidyasagar [3, 4] may be written as

$$f_y = -m \left\{ \ddot{U}_y + \ddot{\theta}(X + d) \right\} \quad , \tag{12b}$$

in other words, the nonlinear term $m\dot{\theta}^2 U_y$ has been omitted. This example indecates that the expressions of the inertia force and gravity obtained in this work contain no approximation and are more general than those obtained in [1, 2, 3, 4].

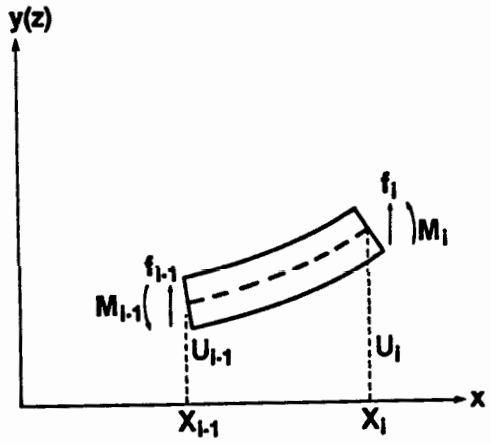

Fig. 3 The Generic i-th Beam Element

FINITE ELEMENT ANALYSIS

The generic i-th beam element connects the (i-1)-th nodal point and the i-th nodal point, as shown in Fig. 3. Based on elementary beam theory, the governing equation of this element may be written as [7, 8, 9]:

$$\mathbf{K}^i \begin{bmatrix} U_{i-1} \\ U_i \\ S_{i-1} \\ S_i \end{bmatrix} = \begin{bmatrix} f_{i-1} \\ f_i \\ M_{i-1} \\ M_i \end{bmatrix} \quad , \tag{13}$$

where the local stiffness matrix of the i-th element is expressed as

$$\mathbf{K}^i = \frac{EI}{l_i^3} \begin{bmatrix} 12 & -12 & 6l_i & 6l_i \\ -12 & 12 & -6l_i & -6l_i \\ 6l_i & -6l_i & 4l_i^2 & 2l_i^2 \\ 6l_i & -6l_i & 2l_i^2 & 4l_i^2 \end{bmatrix} \quad ; \tag{14}$$

E is the Young's modulus; $l_i \equiv X_i - X_{i-1}$; I is the moment of inertia; for the i-th nodal point, U_i is the displacement U_y(U_z), $S_i = dU_i / dX$ is the slope, f_i is the acting force f_y(f_z), M_i is the moment about z (- y)-axis.

The global stiffness matrix of the beam is the assembly of all the local stiffness matrices. The boundary condition of a cantilever beam is that the displacement and the slope are zero at the fixed end. After this boundary condition is imposed, the governing equations for the beam may be expressed as

$$\mathbf{K}_a\mathbf{U} + \mathbf{K}_b\mathbf{S} = \mathbf{f} \quad , \tag{15}$$

$$\mathbf{K}_c\mathbf{U} + \mathbf{K}_d\mathbf{S} = \mathbf{M} \quad . \tag{16}$$

where

$$\mathbf{U} \equiv (U_1, U_2, \cdots U_n)^T \quad ,$$

$$\mathbf{S} \equiv (S_1, S_2, \cdots S_n)^T \quad ,$$

$$\mathbf{f} \equiv (f_1, f_2, \cdots f_n)^T \quad ,$$

$$\mathbf{M} \equiv (M_1, M_2, \cdots M_n)^T \quad .$$

Since there is no moment acting on the beam , i.e. , $\mathbf{M} = 0$, eqn. (16) implies that

$$\mathbf{S} = -\mathbf{K}_d^{-1}\mathbf{K}_c\mathbf{U} \quad . \tag{17}$$

Substituting eqn. (17) into eqn. (15), the following is obtained

$$\mathbf{KU} = \mathbf{f} \quad , \tag{18}$$

where the stiffness matrix, $\mathbf{K}$, can be calculated as

$$\mathbf{K} = \mathbf{K}_a - \mathbf{K}_b\mathbf{K}_d^{-1}\mathbf{K}_c \quad . \tag{19}$$

In view of eqn. (9), eqn. (18) can be rewritten as

$$\ddot{\mathbf{U}} + \mathbf{m}^{-1}\mathbf{KU} = \mathbf{F} \quad , \tag{20}$$

where m is the mass matrix , i.e.,

$$\mathbf{m} = diag.\ \left[m_1, m_2, \cdots m_n \right] \quad ;$$

and F is the vector of forcing terms . If U_i stands for the displacement U_y (U_z) at the i-th nodal point, then F_i stands for the forcing term F_y (F_z) and

$$F_y(i) = -\left[\sin\phi\ddot{\theta} + 2\cos\phi\dot{\phi}\dot{\theta}\right]\left[X_i + d\right] + \dot{\theta}^2 U_y(i) - \left[-\cos\phi\ddot{\theta} + 2\sin\phi\dot{\phi}\dot{\theta}\right] U_z(i) + 2\cos\phi\dot{\theta}\dot{U}_z(i) \quad , \tag{21}$$

$$F_z(i) = -\left[-\ddot{\phi} + \sin\phi\cos\phi\dot{\theta}^2\right]\left[X_i + d\right] - \cos\phi\ddot{\theta}U_y(i) + \left[\cos^2\phi\dot{\theta}^2 + \dot{\phi}^2\right] U_z(i) - 2\cos\phi\dot{\theta}\dot{U}_y(i) - g\sin\phi \quad . \tag{22}$$

It is noticed that, if θ and ϕ are given as functions of time, eqn. (20) can be readily solved by invoking the Runge-Kutta method or other appropriate numerical methods. However, as it will be seen later, θ, $\dot{\theta}$, ϕ, and $\dot{\phi}$ are regarded as state variables and the governing equations for the flexible robot arm as a control problem will be formulated in the next sections .

TARGET

Consider the displacements, $U_y(i)$ and $U_z(i)$, the velocities, $\dot{U}_y(i)$ and $\dot{U}_z(i)$, the joint angles, θ and ϕ , the angular velocities, $\dot{\theta}$ and $\dot{\phi}$, as the state variables of the system. Consider the angular accelerations, $\ddot{\theta}$ and $\ddot{\phi}$, or the torques , T_θ and T_ϕ , as control variables of the system. The purpose of the control is to find the control laws that make the system converge to a steady state which meets certain prescribed requirements. If the solutions are converging, then, as time approaches inifinity, the time derivatives of all the variables approach zero, and

$$\lim_{t\to\infty}\left[\mathbf{U}_y(t), \mathbf{U}_z(t), \theta(t), \phi(t)\right] = \left[\mathbf{U}_y^f, \mathbf{U}_z^f, \theta^f, \phi^f\right] \quad . \tag{23}$$

According to eqn. (20), it is seen that

$$\mathbf{U}_y^f = 0 \quad , \tag{24}$$

$$\mathbf{m}^{-1}\mathbf{KU}_z^f = -g\sin\phi^f \quad . \tag{25}$$

In order for the end effector to reach the given target position (x^t, y^t, z^t) , eqn. (2) becomes

$$\begin{bmatrix} x^t \\ y^t \\ z^t \end{bmatrix} = \begin{bmatrix} \sin\phi^f\cos\theta^f & -\sin\theta^f & -\cos\phi^f\cos\theta^f \\ \sin\phi^f\sin\theta^f & \cos\theta^f & -\cos\phi^f\sin\theta^f \\ \cos\phi^f & 0 & \sin\phi^f \end{bmatrix} \begin{bmatrix} l + d \\ 0 \\ \Delta \end{bmatrix} , \tag{26}$$

which can be rewritten as

$$\theta^f = \theta^t = \tan^{-1}(y^t/x^t) \quad , \tag{27}$$

$$(l + d)^2 + \Delta^2 = (x^t)^2 + (y^t)^2 + (z^t)^2 = (r^t)^2 \quad , \tag{28}$$

$$\cos\phi^f(l+d) + \sin\phi^f\Delta = z^t \quad , \tag{29}$$

where l is the length of the flexible beam, $\Delta \equiv U_z^f(n)$ is the displacement of the end effector. From eqns. (25, 28, 29) , U_z^f, ϕ^f, and d can be determined.

TORQUES

The torque about z-axis, T_θ , and the torque about y'–*axis* , T_ϕ , can be evaluated as

$$T_\theta = \sum_{i=0}^{n}\left[f_x^* y^* - f_y^* x^*\right]_i + \left[I_h + m_h(L_h/2 - d)^2\right](\sin^2\phi\ddot{\theta} + 2\sin\phi\cos\phi\dot{\phi}\dot{\theta}) \quad , \tag{30}$$

$$T_\phi = \sum_{i=0}^{n}\left[f_z^*(x^*\cos\theta + y^*\sin\theta) - z^*(f_x^*\cos\theta + f_y^*\sin\theta)\right]_i + \left[I_h + m_h(L_h/2 - d)^2\right](\ddot{\phi} - \sin\phi\cos\phi\dot{\theta}^2) + m_h g(L_h/2 - d)\sin\phi \quad , \tag{31}$$

where I_h, m_h, and L_h, are the moment of inertia , the mass, and the length of the hub, respectively; x^*, y^*, z^* are the coordinates of the nodal point, which can be calculated by eqn. (2); f_x^*, f_y^*, f_z^* are the forces acting on that nodal point , which can be calculated by eqn. (8).

It is noticed that eqns. (30, 31) are very complicated since the effect of deformation on the torque is incorporated in the formulation. If the effect of deformation on the torques is neglected, then T_θ and T_ϕ are reduced to

$$T_\theta \simeq T_\theta' = (\sin^2\phi\ddot{\theta} + 2\sin\phi\cos\phi\dot{\phi}\dot{\theta})\, I_t \quad , \tag{32}$$

$$T_\phi \simeq T_\phi' = (\ddot{\phi} - \sin\phi\cos\phi\dot{\theta}^2)\, I_t + g\sin\phi\left\{m_h(L_h/2 - d) - \sum_{i=0}^{n} m_i(X_i + d)\right\} \quad , \tag{33}$$

where

$$I_t = \left\{\sum_{i=0}^{n} m_i(X_i + d)^2 + \left[I_h + m_h(L_h/2 - d)^2\right]\right\} \quad .$$

For converging solutions , it is seen that, as time approaches infinity, T_θ and T_θ' approch zero, and

$$\Delta T_\phi \equiv \lim_{t\to\infty}(T_\phi - T_\phi') = \left[\sum_{i=0}^{n} m_i U_z^f(i)\right] g\cos\phi^f \quad , \tag{34}$$

which is a measure of the effect of deformation on the torque in the static case.

If it is feasible to consider $\ddot{\theta}$ and $\ddot{\phi}$ as control variables, then it is straightforward, as it will be seen later, to formulate the control laws; moreover, the torques, T_θ and T_ϕ, can be calculated according to eqns. (30, 31) taking the effect of deformation into consideration. On the other hand, if torques are taken as the control variables and one is willing to make an approximation, i.e., to neglect the effect of deformation on the torques, then eqns. (32, 33) can be expressed as

$$\ddot{\theta} = g_1(\alpha)T_\theta' + g_2(\alpha) \quad , \tag{35}$$

$$\ddot{\phi} = h_1 T_\phi' + h_2(\alpha) \quad , \tag{36}$$

where α stands for all the state variables. Now, eqns. (35, 36) and eqn. (20) form a complete set of governing equations for the control system. However, it is felt that the effect of deformation on the torques should be considered in the treatment for the sake of consistency. In this work, the angular accelerations are taken as the control variables and in the forthcoming paper, the torques, which include the effect of deformation, will be taken as the control variables.

EQUATIONS OF THE SYSTEM

Define two vectors of state variables as follows

$$\alpha_1 \equiv \left[U_y(1), \cdots U_y(n), \theta', \dot{U}_y(1), \cdots \dot{U}_y(n), \dot{\theta} \right], \tag{37}$$

$$\alpha_2 \equiv \left[U_z'(1), \cdots U_z'(n), \phi', \dot{U}_z(1), \cdots \dot{U}_z(n), \dot{\phi} \right], \tag{38}$$

where

$$\begin{aligned} \theta' &\equiv \theta - \theta^f \\ \phi' &\equiv \phi - \phi^f \\ U_z'(i) &\equiv U_z(i) - U_z^f(i) \quad , \quad i = 1, 2, \cdots n. \end{aligned} \tag{39}$$

Then the governing equations of the system can be written as

$$\dot{\alpha}_1 = \mathbf{A}_1\alpha_1 + \mathbf{B}_1 u_1 + \mathbf{N}_1(\alpha_1, \alpha_2, u_1, u_2) \quad , \tag{40}$$

$$\dot{\alpha}_2 = \mathbf{A}_2\alpha_2 + \mathbf{B}_2 u_2 + \mathbf{N}_2(\alpha_1, \alpha_2, u_1, u_2) \quad , \tag{41}$$

where

$$\mathbf{B}_1 = \left[0, 0, \cdots 0, b_1(1), b_1(2), \cdots b_1(n), 1 \right]^T \quad , \tag{42}$$

$$b_1(i) = -\sin\phi^f (X_i + d) + \cos\phi^f U_z^f(i) \quad , \tag{43}$$

$$\mathbf{B}_2 = \left[0, 0, \cdots 0, b_2(1), b_2(2), \cdots b_2(n), 1 \right]^T \quad , \tag{44}$$

$$b_2(i) = X_i + d \quad , \tag{45}$$

$$\mathbf{N}_1 = \left[0, 0, \cdots 0, N_1(1), N_1(2), \cdots N_1(n), 0 \right]^T \quad , \tag{46}$$

$$\begin{aligned} N_1(i) = {} & \left[(\sin\phi^f - \sin\phi)(X_i + d) + \cos\phi U_z(i) - \cos\phi^f U_z^f(i) \right] \ddot{\theta} \\ & + \dot{\theta}^2 U_y(i) + 2\cos\phi\dot{\theta}\dot{U}_z(i) \\ & - 2[\cos\phi(X_i + d) + \sin\phi U_z(i)]\dot{\phi}\dot{\theta} \quad , \end{aligned} \tag{47}$$

$$\mathbf{N}_2 = \left[0, 0, \cdots 0, N_2(1), N_2(2), \cdots N_2(n), 0 \right]^T \quad , \tag{48}$$

$$\begin{aligned} N_2(i) = {} & -\cos\phi U_y(i)\ddot{\theta} \\ & + [\cos^2\phi U_z(i) - \sin\phi\cos\phi(X_i + d)]\dot{\theta}^2 \\ & + U_z(i)\dot{\phi}^2 - 2\cos\phi\dot{\theta}\dot{U}_y(i) \\ & - g[\sin\phi - \sin\phi^f - \cos\phi^f(\phi - \phi^f)] \quad , \end{aligned} \tag{49}$$

$$u_1 = \ddot{\theta} \quad , \tag{50}$$

$$u_2 = \ddot{\phi} \quad , \tag{51}$$

and the nonvanishing components of the two $(2n+2)$x$(2n+2)$ matrices, $\mathbf{A}_1$ and $\mathbf{A}_2$, are

$$\begin{aligned} & (A_1)_{ij} = (A_2)_{ij} = 1, \\ & \qquad 1 \le i \le n+1, \; j = i + n + 1 \quad ; \\ & (A_1)_{ij} = (A_2)_{ij} = (-m^{-1}K)_{ij}, \\ & \qquad 1 \le j \le n, \quad n+2 \le i \le 2n+1 \quad ; \\ & (A_2)_{ij} = -g\cos\phi^f \quad , \\ & \qquad j = n+1, \quad n+2 \le i \le 2n+1 \quad . \end{aligned} \tag{52}$$

From eqns. (40, 41), it is seen that the angular accelerations, $\ddot{\theta}$ and $\ddot{\phi}$, are taken as the control variables; also, all the nonlinear terms are contained in the functions $\mathbf{N}_1$ and $\mathbf{N}_2$ which have the following property

$$\begin{bmatrix} \mathbf{N}_1 \\ \mathbf{N}_2 \end{bmatrix} \to 0 \quad as \quad \begin{bmatrix} \theta(t) \\ \phi(t) \\ U_y(t) \\ U_z(t) \end{bmatrix} \to \begin{bmatrix} \theta^f \\ \phi^f \\ 0 \\ U_z^f \end{bmatrix} \quad . \tag{53}$$

From now on, the governing equations of the system, eqns. (40, 41), may be written symbolically as

$$\dot{\alpha} = \mathbf{A}\alpha + \mathbf{B}u + \mathbf{N}(\alpha_1, \alpha_2, u_1, u_2) \quad . \tag{54}$$

THE MEASUREMENTS

It is assumed that the position of the end effector (x_n^*, y_n^*, z_n^*) can be measured. Recall eqn. (2) and eqn. (26) as follows:

$$\begin{bmatrix} x_n^* \\ y_n^* \\ z_n^* \end{bmatrix} = \mathbf{Q} \begin{bmatrix} l + d \\ U_y(n) \\ U_z(n) \end{bmatrix} \quad , \tag{55}$$

$$\begin{bmatrix} x^t \\ y^t \\ z^t \end{bmatrix} = \mathbf{Q}^f \begin{bmatrix} l + d \\ 0 \\ U_z^f(n) \end{bmatrix} \quad . \tag{56}$$

Then the difference between the position of the end effector and the target position can be obtained as

$$\begin{bmatrix} \Delta x^* \\ \Delta y^* \\ \Delta z^* \end{bmatrix} = \begin{bmatrix} x_n^* - x^t \\ y_n^* - y^t \\ z_n^* - z^t \end{bmatrix} \quad . \tag{57}$$

Define a vector, δ, as follows:

$$\begin{aligned} \delta \equiv \begin{bmatrix} \delta_x \\ \delta_y \\ \delta_z \end{bmatrix} &\equiv (\mathbf{Q}^f)^T \begin{bmatrix} \Delta x^* \\ \Delta y^* \\ \Delta z^* \end{bmatrix} \\ &= (\mathbf{Q}^f)^T \mathbf{Q} \begin{bmatrix} l + d \\ U_y(n) \\ U_z(n) \end{bmatrix} - \begin{bmatrix} l + d \\ 0 \\ U_z^f(n) \end{bmatrix} \quad . \end{aligned} \tag{58}$$

It is seen that δ is a nonlinear function of the state variables. If a Taylor series expansion of δ is performed about the final position, $(\theta = \theta^f, \phi = \phi^f, U_y = 0, U_z = U_z^f)$, the linear expressions of δ_y and δ_z are obtained as

$$\delta_1 \equiv \delta_y \approx \mathbf{H}_1\alpha_1 = U_y(n) + \left[\sin\phi^f (l + d) - \cos\phi^f U_z^f(n) \right] \theta' \quad , \tag{59}$$

$$\delta_2 \equiv \delta_z \approx \mathbf{H}_2\alpha_2 = U_z'(n) - (l + d)\phi' \quad . \tag{60}$$

Now the governing equations and the measurements of the system in linear form can be symbolically written as

$$\dot{\alpha} = \mathbf{A}\alpha + \mathbf{B}u \quad , \tag{61}$$

$$\delta = \mathbf{H}\alpha \quad , \tag{62}$$

where **A**, **B**, **H** are constant matrices (vectors), based on which the estimator will be constructed.

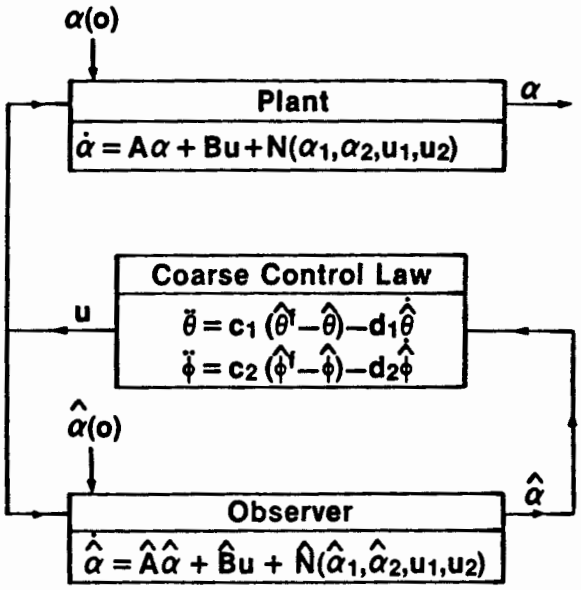

Fig. 4 The Block Diagram of Coarse Control

THE CONTROL

Now, the system (plant) is represented by

$$\dot{\alpha} = \mathbf{A}\alpha + \mathbf{B}u + \mathbf{N}(\alpha_1, \alpha_2, u_1, u_2) \quad , \tag{63}$$

$$\delta = \delta(\alpha) \approx \mathbf{H}\alpha \quad , \tag{64}$$

and, based on **A**, **B**, and **H** , one wishes to construct a controller represented by

$$\dot{\hat{\alpha}} = \hat{\mathbf{A}}\hat{\alpha} + \hat{\mathbf{B}}u + \mathbf{L}(\delta - \hat{\mathbf{H}}\hat{\alpha}) \quad , \tag{65}$$

$$u = -\mathbf{C}\hat{\alpha} \quad , \tag{66}$$

where **C** and **L** are called the control gain and estimate gain, respectively; $\hat{\alpha}$, the estimates of α, are the state variables of the estimator (observer); and, with the symbol "^" on top of **A**, **B**, and **H** , it is emphasized that the number of beam elements, $\hat{n}$, for constructing estimator may be different from (far less than) that for simulating the system. If there had been no nonlinear function, **N**, in eqn. (63) and no difference between $\delta(\alpha)$ and $\mathbf{H}\alpha$ in eqn. (64), then the properly obtained gain matrices (vectors), **C** and **L**, would have guaranteed the convergency and the stability of the solutions, in other words, the end effector eventually would have reached the target position asymptotically. Now, on the contrary, it is noticed that **N** approches zero and δ approaches $\mathbf{H}\alpha$ only if (θ, ϕ, U_y, U_z) approach (θ^f, ϕ^f, 0, U_z^f). Therefore, eqns. (65, 66) may be referred as *fine control*; eqn. (66) is then named the fine control law. As *coarse control* is concerned, which is the first-stage control, eqns. (65, 66) are replaced by

$$\dot{\hat{\alpha}} = \hat{\mathbf{A}}\hat{\alpha} + \hat{\mathbf{B}}u + \hat{\mathbf{N}}(\hat{\alpha}_1, \hat{\alpha}_2, u_1, u_2) \quad , \tag{67}$$

$$\ddot{\theta} = c_1(\hat{\theta}^f - \hat{\theta}) - d_1\dot{\hat{\theta}} \quad , \tag{68}$$

$$\ddot{\phi} = c_2(\hat{\phi}^f - \hat{\phi}) - d_2\dot{\hat{\phi}} \quad , \tag{69}$$

where the last two equations may be named the coarse control laws ; c_1, c_2, d_1, and d_2 are positive constants; the nonlinear function $\hat{\mathbf{N}}$ in eqn. (67) may be omitted. One shifts from coarse control to fine control at time t_1 as soon as the following condition is met

$$| \hat{\theta}(t_1) - \hat{\theta}^f | \le \theta^e \quad , \quad | \hat{\phi}(t_1) - \hat{\phi}^f | \le \phi^e \quad , \tag{70}$$

where θ^e and ϕ^e are input parameters set by the designer of the control system. In this work, $\theta^e = \phi^e = 5^o$.

The control gain and the estimate gain can be calculated by using the pole-placement formulae, first stated by Bass and Gura [10]. The detailed derivations are presented by Friedland [11]. The operational procedures are briefly outlined as follows. First, find the $2\hat{n} + 2$ eigenvalues of the $\hat{\mathbf{A}}$-matrix by solving

$$\det \left[s\mathbf{I} - \hat{\mathbf{A}} \right] = 0 \quad . \tag{71}$$

Since $\hat{\mathbf{A}}$ is a real matrix and damping is not included in this analysis so far, all the eigenvalues are pure imaginary and any eigenvalue's complex conjugate is also an eigenvalue. Furthermore, it is noticed that there are two zero-eigenvalues which are associated with the rigid rotation of the arm. Therefore, the $2\hat{n} + 2$ coefficients of the characteristic polynomial can be found as

$$s^{2\hat{n}+2} + a_1 s^{2\hat{n}+1} + a_2 s^{2\hat{n}} + \cdots + a_{2\hat{n}+2} = s^2 \prod_{i=1}^{\hat{n}} (s^2 + \omega_i^2) \quad , \tag{72}$$

where ω_1 is the largest eigenvalue, ω_2 is the second largest eigenvalue, ... etc. Let the desired eigenvalues of $\hat{\mathbf{A}} - \hat{\mathbf{B}}\mathbf{C}$ and $\hat{\mathbf{A}} - \mathbf{L}\hat{\mathbf{H}}$ be denoted by $-\lambda_i + j\omega_i$ and $-\gamma_i + j\omega_i$, respectively. Then the coefficients of the characteristic polynomials of $\hat{\mathbf{A}} - \hat{\mathbf{B}}\mathbf{C}$ and $\hat{\mathbf{A}} - \mathbf{L}\hat{\mathbf{H}}$ can be found respectively as

$$s^{2\hat{n}+2} + \hat{a}_1 s^{2\hat{n}+1} + \hat{a}_2 s^{2\hat{n}} + \cdots + \hat{a}_{2\hat{n}+2} = (s + \lambda_0)^2 \prod_{i=1}^{\hat{n}} (s + \lambda_i - j\omega_i)(s + \lambda_i + j\omega_i) \quad , \tag{73}$$

$$s^{2\hat{n}+2} + \bar{a}_1 s^{2\hat{n}+1} + \bar{a}_2 s^{2\hat{n}} + \cdots + \bar{a}_{2\hat{n}+2} = (s + \gamma_0)^2 \prod_{i=1}^{\hat{n}} (s + \gamma_i - j\omega_i)(s + \gamma_i - j\omega_i) \quad . \tag{74}$$

It is seen that λ_i (γ_i) are the displacements of the poles. For this work, it is proposed, as a result of experiences, to determine the displacements of the poles by the following formulae

$$\lambda_{2k} = \lambda_{2k-1} = \lambda_0 e^{-\zeta \omega_k / \omega_1} \quad , \tag{75}$$

$$\gamma_{2k} = \gamma_{2k-1} = \gamma_0 e^{-\zeta \omega_k / \omega_1} \quad , \tag{76}$$

where $k = 1, 2, \cdots$ and $2k \le \hat{n}$; λ_0, γ_0, ξ, and ζ are input parameters control gain and the estimate gain can be obtained by using the Bass-Gura formula as

$$\mathbf{C}^T = \mathbf{U}^T\mathbf{W}^T\,(\hat{\mathbf{a}} - \mathbf{a}) \quad , \tag{77}$$

$$\mathbf{L} = \mathbf{V}^T\mathbf{W}^T\,(\bar{\mathbf{a}} - \mathbf{a}) \quad , \tag{78}$$

where

$$\mathbf{W}^{-1} = \begin{bmatrix} 1 & a_1 & a_2 & a_3 & \cdots & a_{2\hat{n}+1} \\ 0 & 1 & a_1 & a_2 & \cdots & a_{2\hat{n}} \\ 0 & 0 & 1 & a_1 & \cdots & a_{2\hat{n}-1} \\ 0 & 0 & 0 & 1 & \cdots & a_{2\hat{n}-2} \\ \cdot & \cdot & \cdot & \cdot & \cdots & \cdot \\ 0 & 0 & 0 & 0 & \cdots & \cdot \\ 0 & 0 & 0 & 0 & \cdots & a_1 \\ 0 & 0 & 0 & 0 & \cdots & 1 \end{bmatrix} \quad , \tag{79}$$

$$\mathbf{U} = \left[\hat{\mathbf{B}},\ \hat{\mathbf{A}}\hat{\mathbf{B}},\ \hat{\mathbf{A}}^2\hat{\mathbf{B}},\ \cdots \hat{\mathbf{A}}^{2\hat{n}+1}\hat{\mathbf{B}}\right]^{-1} \quad , \tag{80}$$

$$\mathbf{V} = \left[\hat{\mathbf{H}}^T,\ \hat{\mathbf{A}}^T\hat{\mathbf{H}}^T,\ (\hat{\mathbf{A}}^T)^2\hat{\mathbf{H}}^T,\ \cdots (\hat{\mathbf{A}}^T)^{2\hat{n}+1}\hat{\mathbf{H}}^T\right]^{-1} \quad . \tag{81}$$

It is noticed that the existence of U and V imply that the system is controllable (controllability) and observable (observability), respectively. The block diagrams of the system and the estimator for coarse control and fine control are shown in Fig.4 and Fig.5, respectively.

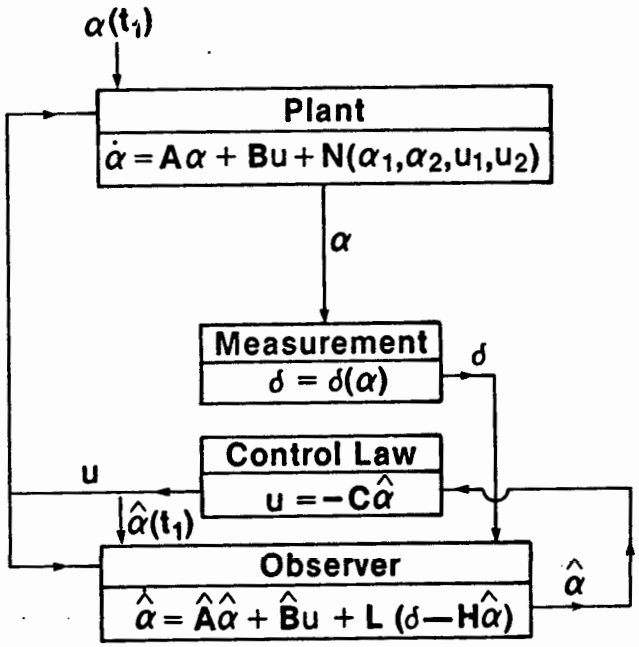

Fig. 5 The Block Diagram of Fine Control

SAMPLING RATE AND DAMPING

Rewrite eqns. (63-66) as follows

$$\dot{\alpha} = \mathbf{A}\alpha - \mathbf{BC}\hat{\alpha} + \mathbf{N}\,(\alpha\,, -\mathbf{C}\hat{\alpha}) \quad , \tag{82}$$

$$\dot{\hat{\alpha}} = (\hat{\mathbf{A}} - \hat{\mathbf{B}}\mathbf{C} - \mathbf{L}\hat{\mathbf{H}})\hat{\alpha} + \mathbf{L}\delta(\alpha) \quad , \tag{83}$$

which are the governing equations for the plant and the observer. In computer simulation, one may solve eqn. (82) and eqn. (83) together by Runge-Kutta method, in other words, the plant and the observer are treated as integral parts of an unified system. On the other hand, one may also rewrite eqns. (82, 83) as

$$\dot{\alpha} = \mathbf{A}\alpha + \mathbf{N}\,(\alpha,\, u\,) + \mathbf{B}u \quad , \tag{84}$$

$$\dot{\hat{\alpha}} = (\hat{\mathbf{A}} - \mathbf{L}\hat{\mathbf{H}})\hat{\alpha} + \hat{\mathbf{B}}u + \mathbf{L}\delta \quad , \tag{85}$$

and, in solving eqn. (84) for α in the time interval $[\,t', t' + \Delta t\,]$, u is regarded as a constant, i.e. ,

$$u = -\mathbf{C}\hat{\alpha}(t') \quad ; \tag{86}$$

and, similarly, in solving eqn. (85) for $\hat{\alpha}$ in the same time interval, u and δ are regarded as constants where

$$\delta = \delta[\,\alpha(t')\,] \quad . \tag{87}$$

In other words, the informations of u and δ are calculated and transmitted to the plant /observer once in a time interval of Δt , hence, Δt and $1/\Delta t$ may be named the transmission time and the sampling rate, respectively. It will be seen later that the sampling rate can not be too small, otherwise the system will become uncontrollable.

The governing equations for the mechanical system, eqn. (20), can be rewitten as

$$\mathbf{m}\ddot{\mathbf{U}} + \mathbf{KU} = \mathbf{mF} \quad , \tag{88}$$

in which damping is not included. Suppose the damping ratio of the structure is experimentally found to be β ($\beta = 0.002$ for steel), what will be the governing equations for the mechanical system including damping ? The answer is

$$\mathbf{m}\ddot{\mathbf{U}} + \mathbf{D}\dot{\mathbf{U}} + \mathbf{KU} = \mathbf{mF} \quad , \tag{89}$$

where D , the damping matrix , is to be constructed as follows . First, solve

$$\det\,(\mathbf{K} - \omega^2\bar{\mathbf{m}}) = 0 \tag{90}$$

to obtain the eigenvalues ω_i and the corresponding eigenvectors $\mathbf{Z}_i$ ($i = 1, 2, \ldots n$). In eqn. (90), $\bar{\mathbf{m}}$ stands for the mass matrix of the structure itself. The eigenvector $\mathbf{Z}_i$ should be orthonormalized to observe the following properties

$$\mathbf{Z}_i^T\bar{\mathbf{m}}\mathbf{Z}_j = \mathbf{Z}_i^T\mathbf{K}\mathbf{Z}_j = 0 \quad , \quad i \ne j$$

$$\mathbf{Z}_i^T\bar{\mathbf{m}}\mathbf{Z}_i = 1 \quad ,$$

$$\mathbf{Z}_i^T\mathbf{K}\mathbf{Z}_i = \omega_i^2 \quad . \tag{91}$$

Then the damping matrix is obtained as

$$\mathbf{D} = 2\beta\bar{\mathbf{m}}\left[\sum_{i=1}^{n}\omega_i\mathbf{Z}_i\mathbf{Z}_i^T\right]\bar{\mathbf{m}} \tag{92}$$

One may prove that D has the following properties

$$\mathbf{Z}_i^T\mathbf{D}\mathbf{Z}_j = 0 \quad , \quad i \ne j$$

$$\mathbf{Z}_i^T\mathbf{D}\mathbf{Z}_i = 2\beta\omega_i \quad . \tag{93}$$

The software developed at NBS does have the capability for the user to decide whether to include damping or not.

NUMERICAL RESULTS

In this section, for illustrative purposes, the results of several cases are presented. Common to all those cases, the following parameters, unless otherwise stated, are set to be

(a) material : aluminum

E=6.895x10^7 kPa ,

$\rho = 0.2713 \times 10^{-2}$ $kg/cm.^3$,

(b) geometry of the flexible arm

$r_o = 1$ *in.* $= 2.54$ *cm* ,

$r_i = 0.9$ *in.* $= 2.286$ *cm* ,

(c) payload

$m^a = 40$ *lbf* $= 177.92$ *Newton* ,

(d) target position

$\theta^t = \phi^t = 45^o$,

(e) initial joint angles

$\theta(0) = 0^o$, $\phi(0) = 90^o$.

(f) number of beam elements

n = 12 (plant)

$\hat{n}$ = 4 (observer)

(g) coarse control parameters

$c_1 = c_2 = 40/sec^2$, $d_1 = d_2 = 40/sec$.

(h) fine control parameters

$\lambda_0 = 25/sec$, $\gamma_0 = 26.25/sec$, $\xi = \zeta = 4$.

In Fig. (6-12), the joint angles $\theta(\phi)$ (solid lines) and the tip angles θ_{tip} (ϕ_{tip}) (solid lines with marks) are shown as functions of time. The tip angles are defined as

$$\theta_{tip} = \tan^{-1}(y_n^*/x_n^*) \tag{94}$$

$$\phi_{tip} = \cos^{-1}(z_n^*/\sqrt{(x_n^*)^2 + (y_n^*)^2 + (z_n^*)^2}) \tag{95}$$

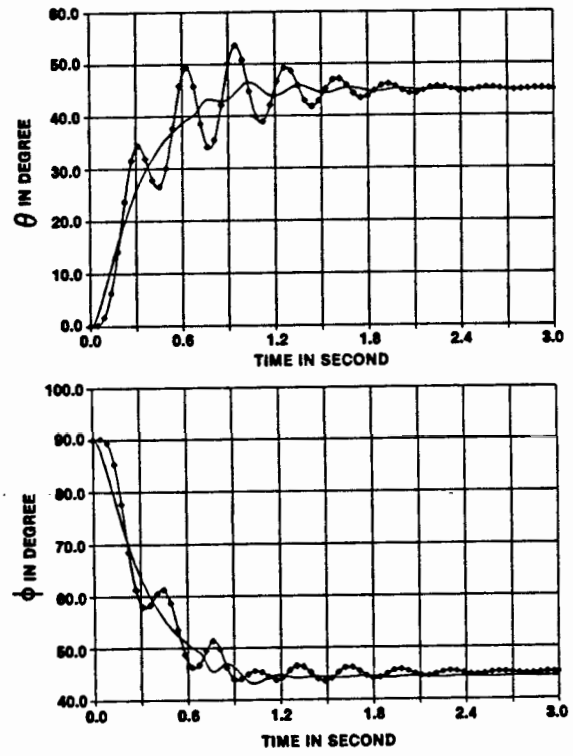

Fig. 6 Responses of joint angles and tip angles ℓ = 60 inches, r_0 = 1 inch, r_1 = 0.9 inch, r^t = 65 inches, $C_1 = C_2$ = 60/sec^2, $d_1 = d_2$ = 20/sec, λ_0 = 25/sec, γ_0 = 26.25/sec, $\xi = \zeta = 4$.

For Fig.6,

$\ell = 60$ *in.* $= 152.4$ *cm* , $r^t = 65$ *in.* $= 165.1$ *cm* ,

$c_1 = c_2 = 60/sec^2$, $d_1 = d_2 = 20/sec$;

and it is noticed the settling time , t_s, is about 3 seconds and $\phi^f = 43.07^o$, the ratio of payload with respect to the weight of the flexible arm, R, is about 11.4 .

For Fig.7 (Fig.8),

$\ell = 120$ *in.* $= 304.8$ *cm* (240 *in.* $= 609.6$ *cm*) ,

$r^t = 130$ *in.* $= 330.2$ *cm* (250 *in.* $= 635.0$ *cm*) ,

$\phi^f = 42.3^o$ (34.8^o) ,

$R = 5.7$ (2.85) ,

$t_s = 4.2$ *sec.* (5.0 *sec.*) .

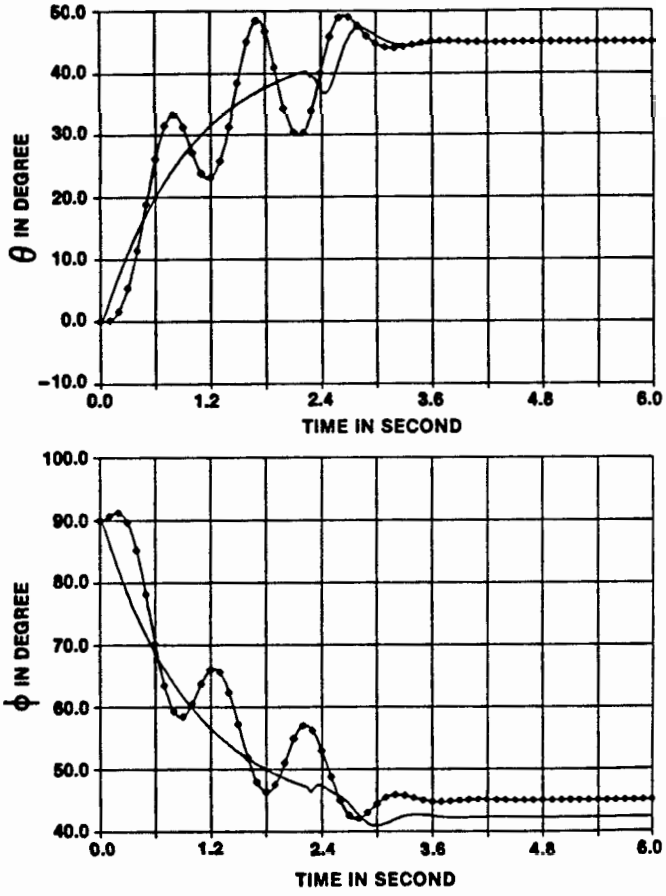

Fig. 7 Responses of joint angles and tip angles ℓ = 120 inches, r_0 = 1 inch, r_1 = 0.9 inch, r^t = 130 inches, $C_1 = C_2$ = 40/sec^2, $d_1 = d_2$ = 40/sec, λ_0 = 25/sec, γ_0 = 26.25/sec, $\xi = \zeta = 4$.

In Fig.9 (Fig.10), the length of the flexible arm and the r-coordinate of the target are increased respectively to

$\ell = 360$ *in.* $= 914.4$ *cm* (600 *in.* $= 1524.0$ *cm*) ,

$r^t = 370$ *in.* $= 939.8$ *cm* (620 *in.* $= 1574.8$ *cm*) ;

the outer radius and the inner radius of the arm are increased to $r_o = 2\ in. = 5.08\ cm$ and $r_i = 1.9\ in. = 4.826\ cm$ while the thickness of the cylinder still kept at 0.1 inch = 0.254 cm ; and other parameters are changed to :

$$c_1 = c_2 = 40/sec^2 \quad (\ 10/sec^2\ )\ ,$$

$$\lambda_0 = 25/sec \quad (\ 10/sec\ )\ ,$$

$$\gamma_0 = 26.25/sec \quad (\ 10.5/sec\ )\ ;$$

and it is found that

$$\phi^f = 41.2^o \quad (\ 34.2^o\ )\ ,$$

$$R = 0.925 \quad (\ 0.555\ )\ ,$$

$$t_s = 5\ sec. \quad (\ 20\ sec.\ )\ .$$

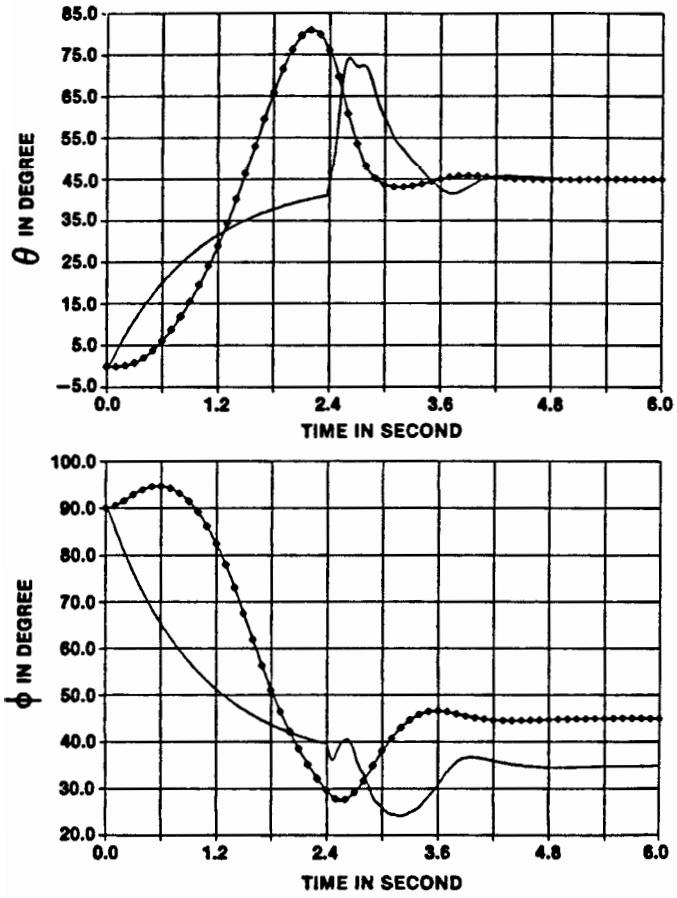

Fig. 8 Responses of joint angles and tip angles
ℓ = 240 inches, r_g = 1 inch, r_l = 0.9 inch, r^t = 250 inches, $C_1 = C_2 = 40/sec^2$, $d_1 = d_2 = 40/sec$, $\lambda_0 = 25/sec$, $\gamma_0 = 26.25/sec$, $\xi = \zeta = 4$.

For all those above-mentioned cases, the plant and the observer are treated as integral parts of an unified system, in other words, the sampling rate is very large. In order to investigate the effect due to the sampling rate, the solutions corresponding to those in Fig.10 are shown in Fig.11 except that the sampling rate is now equal to 100/sec (Δt = 10 msec.). Comparing Fig.10 with Fig.11, the differences in solutions, including the settling time, are noticeable. It has been tried to reproduce the solutions corresponding to those in Fig.8 by setting Δt = 10 msec and Δt = 5 msec . Both attempts failed to yield a converging solution. Finally, by setting Δt = 4 msec, i.e. , sampling rate = 250/sec, a converging solution is obtained and shown in Fig.12, in which it is seen that the settling time is increased from 5 seconds to 10 seconds.

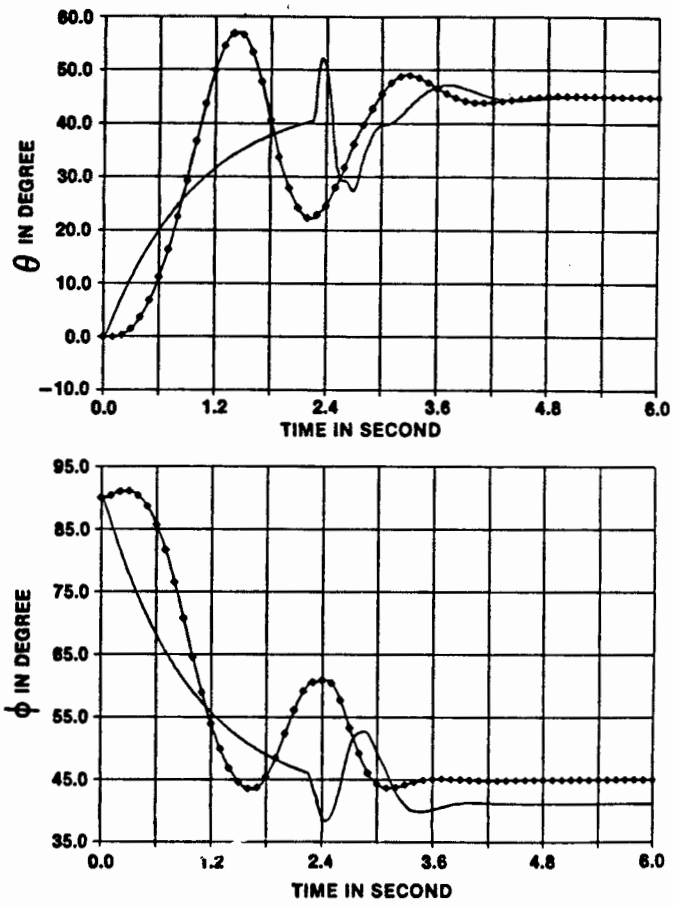

Fig. 9 Responses of joint angles and tip angles
ℓ = 360 inches, r_g = 2 inches, r_l = 1.9 inches, r^t = 370 inches, $C_1 = C_2 = 40/sec^2$, $d_1 = d_2 = 40/sec$, $\lambda_0 = 25/sec$, $\gamma_0 = 26.25/sec$, $\xi = \zeta = 4$.

DISCUSSION

In this work, the single-link flexible robot arm has two degrees of freedom for rotations (θ and ϕ) and one degree of freedom for sliding (d) so that the space, which can be reached by the end effector, is three- dimensional. In the analysis, θ and ϕ are treated as variables, but the sliding, d, is treated as a parameter, i.e. , a constant determined by the given target position.

The governing equations of the system (plant) and the equations representing the measurements, which have been derived rigorously, are nonlinear. No attempt whatsoever has been made to linearize those equations. However, the estimator (observer) was constructed based on the linear version of the system. Also, it is noticed that number of beam elements used to model the plant, n, and the observer, $\hat{n}$, may be different, for example, for those cases reported in this work, n = 12 and $\hat{n}$ = 4. This means the observer is linear and involves very few variables. For practical purpose, it implies that real-time control of flexible robot arm is feasible.

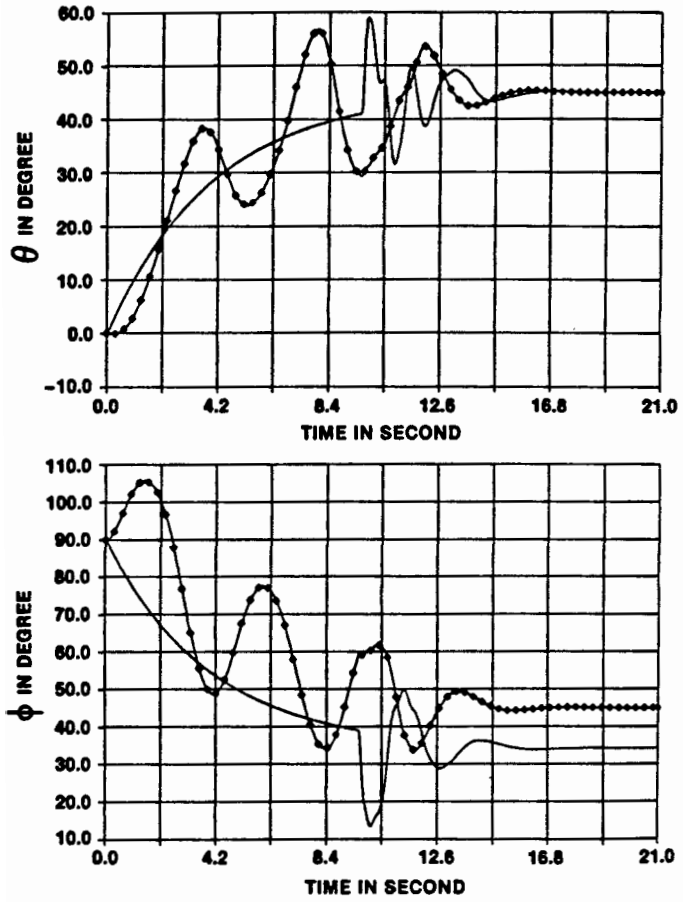

Fig. 10 Responses of joint angles and tip angles
ℓ = 600 inches, r_g = 2 inches, r_l = 1.9 inches, r^4 = 620 inches, $C_1 = C_2$ = 10/sec^2, $d_1 = d_2$ = 40/sec, λ_0 = 10/sec, γ_0 = 10.5/sec, $\xi = \zeta$ = 4.

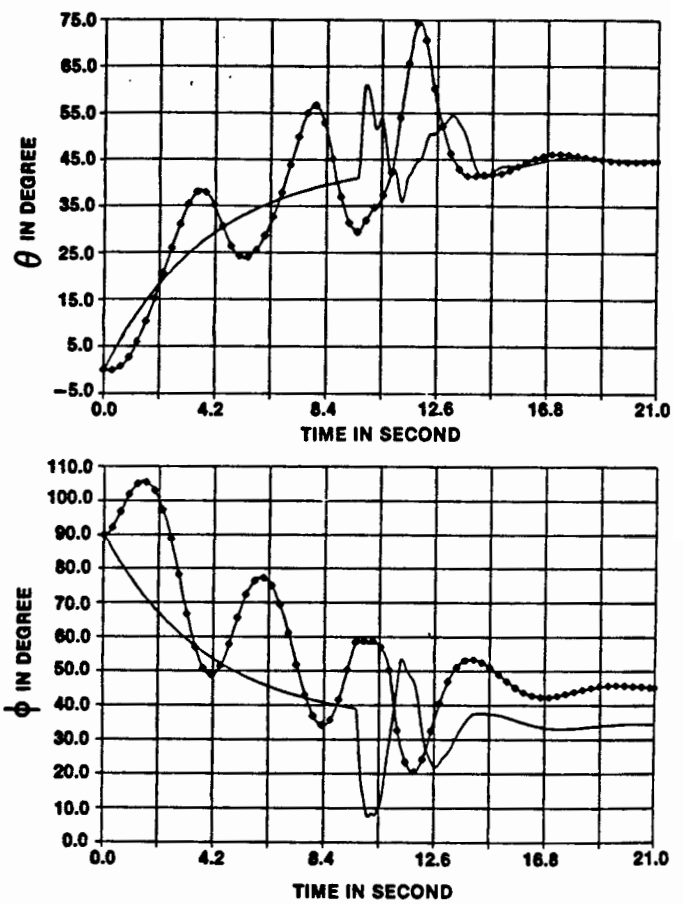

Fig. 11 Responses of joint angles and tip angles
ℓ = 600 inches, r_g = 2 inches, r_l = 1.9 inches, r^4 = 620 inches, $C_1 = C_2$ = 10/sec^2, $d_1 = d_2$ = 40/sec, λ_0 = 10/sec, γ_0 = 10.5/sec, $\xi = \zeta$ = 4, Δt = 10 msec.

If damping is included in the system, one may prove that even a very simple coarse control law serves the purpose to control the flexible robot arm by setting the joint angles at pre-calculated values and letting nature (in this case, damping) take its course. However, the settling time is too long to be practical. On the other hand, as it becomes clear in this study, the combination of the coarse control and the fine control works even if the system has no damping at all. Generally speaking, as it has been pointed out by Book et al [6], damping in the robot arm made of most practical materials, is influential on higher modes, but not on the dominant mode of the arm. It is suggested that engineers do not count on damping for the purpose of controlling the flexible robot arm.

One of the significant findings in this study is that the sampling rate (or the transmission time) is very crucial in the control system. If the sampling rate is reduced too much, then the solution becomes unstable, i.e. , the system is no longer controllable. This phenomenon has been reflected in the numerical results of a couple cases discussed in the previous section.

REFERENCES

1. R. H. Cannon, Jr. and E. Schmitz, "Initial Experiments on the End-Point Control of a Flexible One-link Robot ", International J. of Robotics Reseach, v. 3, 1984, pp. 62-75.
2. F. Harashima and T. Ueshiba, "Adaptive Control of Flexible Arm Using the End-Point Sensing ", Proceedings, Japan-U.S.A. symposium on Flexible Automation, Osaka, Japan, July, 1986, pp. 225-229.
3. D. Wang and M. Vidyasagar, "Modelling and Control of a Flexible Beam Using the Stable Factorization Approach", Proceedings of the 1986 ASME Winter Conference, To appear (private communication)
4. D. Wang and M. Vidyasagar, "Control of a Flexible Beam for Optimum Step Response", Proceedings of the 1986 ASME Winter Conference, To appear (private communication)
5. V. Sangveraphunsiri, "The Optimal Control and Design of a Flexible Manipulator Arm ", Thesis, School of Mechanical Engineering, Georgia Institute of Technology, Atlanta, Ga, 1984.

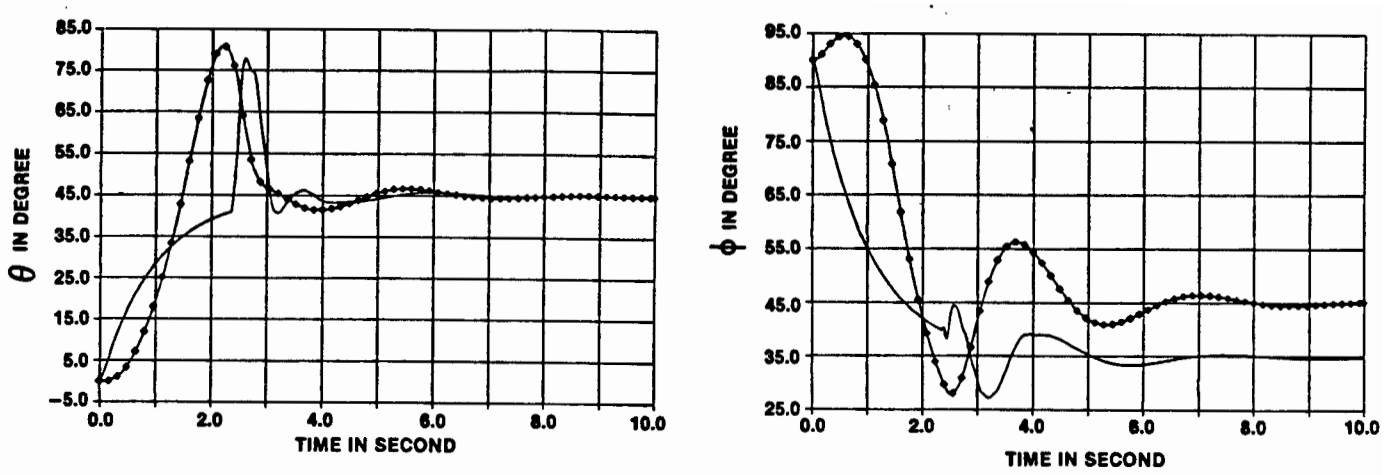

Fig. 12 Responses of joint angles and tip angles
ℓ = 240 inches, r_e = 1 inch, r_l = 0.9 inch, r^t = 250 inches,
$C_1 = C_2 = 40/sec^2$, $d_1 = d_2 = 40/sec$, $\lambda_0 = 25/sec$,
$\gamma_0 = 26.25/sec$, $\xi = \zeta = 4$, $\Delta t = 4$ msec.

6. W. J. Book, T. E. Alberts, and G. G. Hastings, "Design Strategies for High-Speed Lightweight Robot", Computers in Mechanical Engineering, September, 1986, pp. 26-33.
7. J. S. Przemieniecki, Theory of Matrix Structural Analysis, McGraw-Hill Book Co. , New York, 1968.
8. P. Tong and J. N. Rossettos, Finite-Element Method Basic Technique and Implementation, The MIT press, Cambridge, Mass. , 1977.
9. F. L. Stansa, Applied Finite Element Analysis for Engineers, Holt, Rinehart and Winston, New york, 1985.
10. R. W. Bass and I. Gura, "High-Order System Design Via State-Space Considerations", Proc. Joint Automatic Control Conferance, Troy, N.Y. , June 1965, pp. 311-318.
11. B. Friedland, Control System Design An Introduction to State-Space Methods, McGraw-Hill Book Co. , New York, 1986.